Investigation of the DsbA Mechanism through the Synthesis and Analysis of an Irreversible Enzyme−Ligand Complex[†]

Joël Couprie,[‡] Floriana Vinci,[§] Christophe Dugave,[‡] Eric Quéméneur,*[,‡] and Mireille Moutiez[‡]

CEA/Saclay, Département d'Ingénierie et d'Etudes des Protéines, Gif-sur-Yvette, France, and Centro Internazionale di Servizi di Spettrometria di Massa, CNR, Università di Napoli "Federico II", Napoli, Italy

Received December 15, 1999; Revised Manuscript Received April 3, 2000

ABSTRACT: Approaching the molecular mechanism of some enzymes is hindered by the difficulty of obtaining suitable protein−ligand complexes for structural characterization. DsbA, the major disulfide oxidase in the bacterial periplasm, is such an enzyme. Its structure has been well characterized in both its oxidized and its reduced states, but structural data about DsbA−peptide complexes are still missing. We report herein an original, straightforward, and versatile strategy for making a stable covalent complex with a cysteine−homoalanine thioether bond instead of the labile cystine disulfide bond which normally forms between the enzyme and polypeptides during the catalytic cycle of DsbA. We substituted a bromohomoalanine for the cysteine in a model 14-mer peptide derived from DsbB (PID-Br), the membrane partner of DsbA. When incubated in the presence of the enzyme, a selective nucleophilic substitution of the bromine by the thiolate of the DsbA Cys_{30} occurred. The major advantage of this strategy is that it enables the direct use of the wild-type form of the enzyme, which is the most relevant to obtain unbiased information on the enzymatic mechanism. Numerous intermolecular NOEs between DsbA and PID could be observed by NMR, indicating the presence of preferential noncovalent interactions between the two partners. The thermodynamic properties of the DsbA−PID complex were measured by differential scanning calorimetry. In the complex, the values for both denaturation temperature and variation in enthalpy associated with thermal unfolding were between those of oxidized and reduced forms of DsbA. This progressive increase in stability along the DsbA catalytic pathway strongly supports the model of a thermodynamically driven mechanism.

Most of the proteins exported out of the cytosol of prokaryotes and eukaryotes contain disulfide bonds, which are involved in the stabilization of the tertiary structure. In vivo, disulfide bond formation is a catalyzed process, predominantly controlled by enzymes of the thiol/disulfide oxidoreductase family, structurally related to thioredoxin. All these enzymes, among which are PDI and bacterial Dsb enzymes, display a Cys-Xaa-Xaa-Cys sequence which participates in direct thiol−disulfide exchange reactions with protein substrates.

DsbA acts as the main catalyst of disulfide bond formation in the periplasm of *E. coli* (*1*−*3*). This protein has been thoroughly studied in recent years as the most potent oxidase yet known in the thioredoxin family (*4*). The active site sequence of DsbA, Cys-Pro-His-Cys (*5*), is found at positions 30−33 at the amino-terminal end of a α-helix. The thiol of Cys_{30} is accessible to the solvent and acts as a nucleophile in the thiol−disulfide reaction, while the thiol of Cys_{33} is buried in the interior of the protein (*6*, *7*). The reaction with substrates proceeds in two steps and involves a transient enzyme−substrate mixed disulfide intermediate (*8*). The high nucleophilicity of Cys_{30}, resulting both from an unusually low pK_a (around 3.5) and its high accessibility, makes this exchange reaction with protein substrates extremely rapid and efficient (*9*, *10*). The second active site cysteine helps substrate release at the second step of the process (Scheme 1). In vivo, reduced DsbA is then recycled through another mixed disulfide intermediate with a cysteine of the integral membrane DsbB (*11*).

Although many studies have been carried out on both oxidized and reduced forms of the protein, more information remains to be collected to get a complete picture of the catalytic cycle. In particular, the transient nature of the DsbA−substrate disulfide intermediates prevents their accumulation and makes their study difficult. Therefore, a prerequisite to a complete description of the DsbA mechanism is to find a way to stabilize the reaction intermediate.

The first way to stabilize a DsbA−substrate complex has been to replace the second active site cysteine with another residue to prevent the second step of the catalytic cycle. The use of the variants C33Y (*12*) and C33S (*13*) allowed the identification of the DsbB cysteine forming the mixed disulfide with DsbA. This approach was also used in the only attempts to characterize a DsbA−substrate complex (*8*, *14*). Using a complex between the C33A DsbA variant and a variant of RNase T1, Frech and co-workers provided strong evidence of the presence of noncovalent interactions between

[†] Supported by Grant BIO4-CT 96 0436 from the Biotechnology Program of the European Commission.

* Correspondence should be addressed to this author at CEA, Département d'Ingénierie et d'Etudes des Protéines, Bâtiment 152, C.E. de Saclay, F-91191 Gif-sur-Yvette, France. Tel: (33) 1 69 08 76 48, Fax: (33) 1 69 08 90 71, E-mail: eric.quemeneur@cea.fr.

[‡] CEA, Département d'Ingénierie et d'Etudes des Protéines.

[§] Università di Napoli "Federico II".

10.1021/bi992873f CCC: $19.00
Published on Web 05/12/2000

Scheme 1: Catalytic Cycle of DsbA

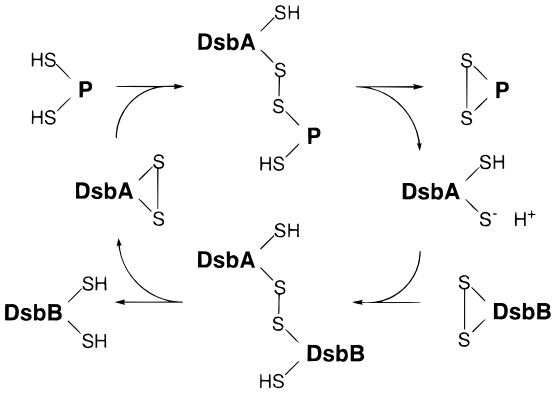

Scheme 2: Site-Directed Alkylation of DsbA Active Site Using the Brominated Peptide PID-Br

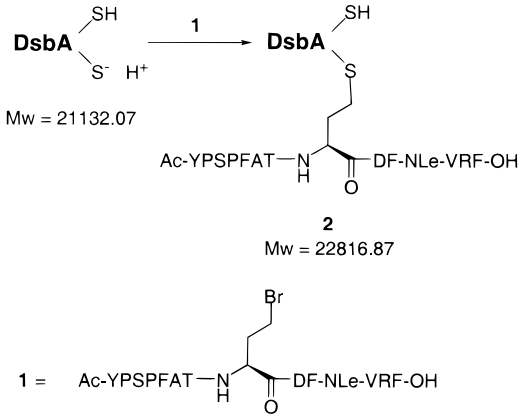

an unfolded polypeptide chain and DsbA in addition to the covalent disulfide bond. However, this kind of linkage proved unsuitable for more detailed structural analyses since the complex was cleaved into its constituents within a few days (*14*). Moreover, such a DsbA variant does not possess the two redox states of the wild-type protein, which constitutes a major drawback for the fine analysis of the molecular events of the mechanism.

All the reasons mentioned above led us to explore an alternative way to obtain a stable DsbA−substrate complex based on the creation of a specific irreversible linkage between the wild-type enzyme and a ligand analogue. The well-known ability of thiols to react readily with electrophiles such as iodoacetamide prompted us to synthesize a novel electrophilic compound. This molecule was designed for interacting in both a specific and an irreversible way with the DsbA active site via the formation of a thioether linkage (Scheme 2). We anticipated that only Cys_{30} would react with the electrophile due to its very low pK_a and its high accessibility to the solvent.

As a ligand, we focused on a peptide derived from DsbB, which was shown to interact specifically with DsbA at the level of Cys_{104} (*12*, *13*). We selected the 14 amino acid sequence Tyr_{97}−Phe_{110} centered on this cysteine. Its highly hydrophobic content suggested moreover that this peptide could specifically interact with the putative hydrophobic peptide-binding site of DsbA (*6*, *7*). To optimize the similarity to DsbB, the peptide was acetylated on the N-terminal residue, and the C-terminal carboxylic function was kept free to mimic the side chain of the close Glu_{112}. A homoalanine cation equivalent, 4-bromohomoalanine, able to react with thiols, was substituted for the cysteine residue occurring in the ligand peptide. As a matter of fact, the *S*-cysteinylhomoalanyl motif may be proposed as a mimic for the cystine, except it does not reproduce the *cisoid/transoid* isomerism (*15*, *16*) (Scheme 2). Moreover, it is resistant to acidic and basic hydrolysis, proteolytic degradation, and most reducing agents (*17*, *18*). The Met_{107} residue of DsbB was replaced by an isosteric norleucine to prevent any side reaction between the sulfur atom and the reagents used for the synthesis of the brominated ligand.

In this paper, we report the synthesis of a DsbB-derived peptide (PID)[1] and the formation and characterization of its complex with DsbA. Calorimetric studies performed on oxidized, complexed, and reduced forms of DsbA highlight the existence of a thermodynamic downward driving force in the mechanism of DsbA. The presence of noncovalent interactions between the protein and its ligand is also demonstrated by NMR. A comparison between the binding properties of the hydroxyl and the thiol form of PID, PID-OH and PID-SH, respectively, will be discussed in order to know whether these interactions precede or follow the formation of the covalent linkage.

MATERIALS AND METHODS

All amino acids, resin, and coupling reagents were purchased from Novabiochem. Tetrahydrofuran was dried over sodium/benzophenone. Circular dichroism measurements were performed with a Jobin Yvon CD6 dichrograph. UV absorptions were measured with a Hewlett-Packard 8453 spectrophotometer.

Peptide Synthesis. (A) Resin-Bound PID-OH. The peptide was synthesized by the standard Fmoc strategy using an Applied Biosystems 431A automatic synthesizer. A 0.1 mmol sample of Fmoc-Phe-Wang resin (0.51 mmol/g) was used. Protective groups were as follows: OtBu (Asp), tBu (Ser, Thr, Tyr), Pmc (Arg), and trityl (Hse). Fmoc groups were deprotected using a mixture of 20% piperidine in *N*-methylpyrrolidone. Deprotection was monitored by UV spectrophotometry. Single-step coupling was performed using *N*,*N*′-dicyclohexylcarbodiimide/*N*-hydroxybenzotriazole in *N*-methylpyrrolidone with a 10-fold excess of protected amino acid. Residual free amines were capped with acetic anhydride. An aliquot of the peptide was analyzed as follows: cleavage from the resin and simultaneous deprotection of the side chains were achieved by treatment with a mixture of TFA/triisopropylsilane/water (9/0.5/0.5) for 1.5 h at room temperature. The crude peptide was precipitated, washed 3 times with diethyl ether, and solubilized in a

[1] Abbreviations: CAM, carboxamidomethyl; DQF-COSY, double-quantum-filtered correlated spectroscopy; DTT, dithiothreitol; EDTA, ethylenediaminetetraacetic acid; ESIMS, electrospray ionization mass spectrometry; [F1-C/N,F2-C/N]-NOESY, NOESY with ^{13}C- and ^{15}N-filtering in the F1 and F2 dimensions; GdmCl, guanidinium chloride; HS-DSC, high-sensitivity differential scanning calorimetry; HSQC, heteronuclear single quantum correlation; MALDIMS, matrix-assisted laser desorption ionization mass spectrometry; NOESY, nuclear Overhauser effect spectroscopy; PID, peptide derived from the DsbB sequence; PID-OH, PID-SH, and PID-Br, respectively homoserine, cysteine, or 4-bromohomoalanine at position 8; Pmc, 2,2,5,7,8-pentamethylchroman-6-sulfonyl; ROESY, rotating frame Overhauser effect correlated spectroscopy; TFA, trifluoroacetic acid; TOCSY, total correlation spectroscopy; TSPd4, 3-trimethylsilyl [2,2,3,3-^2H]propionate.

mixture of acetonitrile/0.1% TFA (40/60). Purity was assessed by HPLC on a SMART system (Pharmacia Biotech) using a μRPC C2/C18 SC 2.1/10 column (Pharmacia Biotech) with the following linear gradient: acetonitrile/0.1% TFA (5/95; 6 min) and then acetonitrile/0.1% TFA (100/0; 19 min) (flow rate: 200 μL/min). PID-OH: $t_r = 14.6$ min; MALDI $m/z = 1703.4$ (MH^+). The sequence of the peptide was assessed by MS/MS analysis and enzymatic proteolysis followed by electrospray analysis.

(B) Synthesis of PID-Br. The peptide grafted on the resin was treated by repeated cycles of 2 min washing with a mixture of TFA/triisopropylsilane/dichloromethane, 1/5/94 (10 mL) (*19*). The deprotection of the trityl group, monitored by UV spectrophotometry, was repeated until completion. The resin was swollen in tetrahydrofuran (2.5 mL), and bromination was achieved with carbon tetrabromide (10 equiv) and triphenylphosphine (10 equiv), 3 h at room temperature. The precipitate was eliminated by washing the resin with tetrahydrofuran, dichloromethane, and methanol. Final deprotection and cleavage of the peptide, performed using a mixture of TFA/water, 95/5, 1.5 h at room temperature, yielded PID-Br which was precipitated as described above and freeze-dried. The purity of the peptide was checked as previously reported. PID-Br: $t_r = 15.8$ min; MALDI $m/z = 1766.1$ (MH^+).

(C) Synthesis of PID-SH. The PID-SH peptide was synthesized in the same way as PID-OH except for the use of trityl-Cys instead of trityl-Hse at cycle 7. After TFA deprotection and cleavage, the peptide was purified by HPLC and analyzed by ESIMS ($m/z = 1661.25$).

Formation of the Complex DsbA−Peptide. All buffers were filtered and degassed before use. DsbA was overexpressed and purified as previously described (*9*): anion exchange chromatography on DEAE-Sephacel (Pharmacia Biotech) followed by hydrophobic chromatography on phenyl-Sepharose CL-4B (Pharmacia Biotech). DsbA concentrations were determined spectrophotometrically using an absorption coefficient of $A_{280,1mg/mL,1cm} = 1.10$ (*9*).

The brominated peptide was solubilized at a concentration of 1 mM in methanol just before use. DsbA active site disulfide was reduced by incubating the enzyme (1−3 mM) with 10 equiv of DTT in 20 mM sodium phosphate buffer, pH 5.5, under argon for 1 h. DTT was removed by gel filtration on a fast-desalting HR 10/10 column (Pharmacia Biotech), using an isocratic gradient with 20 mM sodium phosphate buffer, pH 5.5. The reduced protein (30 μM) was immediately incubated under argon with 2 equiv of brominated peptide in the sodium phosphate buffer previously described containing 30% CH_3OH at 4 °C. After 3 h, 2 further equiv of peptide was added, and the reaction was pursued for 24 h. Complex formation was monitored by SDS−PAGE electrophoresis (12% polyacrylamide). The mixture was further concentrated and the excess of peptide removed by ultrafiltration and successive washes with the reaction buffer on a Centricon-plus 20 (cutoff 10 kDa) (Millipore).

The reaction medium was then dialyzed against a 20 mM Tris-HCl buffer, pH 8, containing 2 M ammonium sulfate, and submitted to hydrophobic chromatography on a phenyl-Sepharose HP column (Pharmacia Biotech) at 4 °C. The elution system consisted of A: 20 mM Tris-HCl, pH 8, 1 M ammonium sulfate; and B: 20 mM Tris-HCl, pH 8. Proteins were purified with a linear gradient from 100% to 20% A in 165 min, 20% A for 35 min, and 20% to 0% A in 165 min at 0.3 mL/min. Fractions were analyzed by SDS−PAGE. Fractions containing pure complex were pooled, dialyzed against 20 mM sodium phosphate, pH 5.8, 0.02% sodium azide, and concentrated successively with Centricon-Plus 20 (cutoff = 10 kDa) from Millipore, Centricon-10, and Microcon (Amicon) up to 2 mM.

Mass Spectrometry Analyses. (A) MALDIMS Analyses. Peptides PID-OH and PID-Br were analyzed by MALDI-TOF mass spectrometry using a Voyager DE mass spectrometer (Perseptive Biosystem). The mass range was calibrated using bovine insulin (average molecular mass 5734.6 Da) and a matrix peak (379.1 Da) as internal standards. Samples were dissolved in methanol at 10 pmol/μL. Then 1 μL was applied to a sample slide and allowed to air-dry, before applyication of 1 μL of α-cyano-4 hydroxycinnamic acid (10 mg/mL) in ethanol/acetonitrile/0.1% TFA, 1/1/1 (v/v/v). The matrix was allowed to air-dry before collection of spectra. Mass spectra were generated from the sum of 50 laser shoots.

(B) ESIMS Analyses. ESIMS and MS/MS analyses were carried out using a Bio-Q triple quadrupole mass spectrometer equipped with an electrospray ion-source (Micromass). The protein solution (10 pmol/μL in 1% acetic acid/50% acetonitrile) was injected directly into the ion source by the Harward apparatus using a flow rate of 5 μL/min. Data were acquired at 10 s/scan and elaborated by Mass Lynx software (Micromass). Mass scale calibration was performed by means of multiply charged ions from a separate injection of horse heart myoglobin (average molecular mass 16951.5 Da).

Protein Denaturation, Reduction, and Carboxamidomethylation. Protein denaturation was performed in 0.1 M Tris-HCl, 1 mM EDTA, pH 8.5, 6 M guanidinium chloride (GdmCl). Protein samples were incubated overnight at 30 °C. Protein reduction, both for native and for denatured protein, was performed in 0.1 M Tris-HCl, 1 mM EDTA, pH 8.5, using a 50-fold molar excess of DTT over the number of cysteine residues for 2 h at 37 °C under an argon atmosphere.

The carboxamidomethylation, for both native and denatured protein, was performed in 0.1 M Tris-HCl, 1 mM EDTA, pH 8.5, using a 10-fold molar excess of iodoacetamide over the number of cysteine residues. The reaction was performed for 20 min at room temperature in the dark to minimize photolytic production of iodine, a very potent oxidizing agent for thiols. The samples were then desalted by reverse-phase HPLC using a Vydac C4 column (5 μm, 0.46 × 25 cm). The elution system consisted of 0.1% TFA (solvent A) and 0.07% TFA in 95% acetonitrile (solvent B). Proteins were desalted with a linear gradient of solvent B from 15% to 95% at a flow rate of 1 mL/min. Eluted compounds were monitored at 220 nm, recovered, and freeze-dried.

NMR Experiments. All experiments were carried out on Bruker DRX-600 or DRX-800 MHz spectrometers using a triple-resonance 5 mm inverse probe equipped with triple axes pulsed-field gradients.

For PID-OH peptide analysis, 3.5 mg of purified peptide was dissolved in 200 μL of CD_3OH and diluted in 20 mM sodium phosphate buffer, pH 5.8, to a volume of 500 μL, yielding a final concentration of 2 mM. The sample also

contained 0.4 mM TSPd4 as internal reference. The following two-dimensional experiments were performed at 288 and 303 K: a pulsed-field gradient DQF-COSY (*20*), a sensitivity-improved TOCSY (*21*) using a 80 ms dipsi-2 mixing sequence (*22*), a NOESY (*23*) with a 120 ms NOE mixing period, and an off-resonance ROESY (*24, 25*) with a 100 ms mixing time and a 54.7° spin-lock angle. For carbon assignments, a sensitivity-enhanced gradient ^{1}H-^{13}C HSQC (*26*) at natural abundance was also recorded. ^{13}C chemical shifts obtained from the ^{1}H-^{13}C HSQC spectrum were used to resolve ^{1}H resonance overlaps occurring in homonuclear spectra between ^{1}Hα and ^{1}Hβ of Thr$_7$, and between ^{1}Hγ and ^{1}Hδ of Nle$_{11}$. ^{13}Cα and ^{13}Cβ chemical shift values, which are characteristic of the residue type (*27*), confirmed the assignments. ^{1}Hα and ^{13}Cα chemical shift deviations from random coil values for the PID-OH were calculated using the Wishart et al. database (*28, 29*) and implementing corrections for residues followed by a proline (*30*).

For experiments on the complex, uniformly ^{15}N- and ^{15}N/^{13}C-labeled DsbA were obtained as described previously (*31*), and the complex was formed between labeled DsbA and the unlabeled PID-Br as described above. NMR samples of oxidized and complexed DsbA contained 2 mM protein, 90% H_2O/10% D_2O, 20 mM sodium phosphate, pH 5.8, 0.4 mM TSPd4. A sample of doubly ^{15}N/^{13}C-labeled DsbA-unlabeled peptide complex dissolved in D_2O was prepared by freeze-drying, resuspension in 99.9% D_2O (Euriso-top), and incubation for 2 days at 310 K. This procedure was repeated 2 times. All experiments were performed at 310 K. Two-dimensional sensitivity-enhanced gradient ^{1}H-^{15}N HSQC spectra (*26*) were recorded for both oxidized and complexed ^{15}N-labeled DsbA. For the selective observation of PID resonances in the complex, two-dimensional doubly isotope filtered [F1-C/N,F2-C/N]-NOESY (*32*) and ^{13}C double-tuned [F1,F2] pulsed-field gradient z-filtered NOESY (*33*) experiments were recorded on doubly labeled samples dissolved in H_2O and D_2O, respectively. For the detection of intermolecular NOEs between labeled DsbA and the unlabeled peptide, a three-dimensional F1 ^{13}C-edited−F3 ^{13}C-filtered HSQC NOESY (*33, 34*) spectrum was recorded at 800 MHz on a sample dissolved in D_2O. In these last three experiments, the NOE mixing time was set to 120 ms.

For samples dissolved in H_2O, the water resonance was suppressed using a WATERGATE suppression scheme (*35*) in all experiments, except those employing pulsed-field gradients for coherence pathway selection. In HSQC experiments, heteronuclear decoupling during acquisition was achieved with the use of a GARP decoupling sequence (*36*). Quadrature detection in the indirectly detected dimensions was obtained by States-TPPI (*37*). Two-dimensional spectra were recorded with 512 (t1) × 2048 (t2) data points (1024 × 4096 for DQF-COSY). Spectral widths of 5682 Hz for the free peptide and 8500 Hz for the complex were used for the proton dimensions. Values of 9000 and 2000 Hz were used for carbon and nitrogen dimensions, respectively. The three-dimensional F1 ^{13}C-edited−F3 ^{13}C-filtered HSQC NOESY was acquired with 80 (t1) × 140 (t2) × 1024 (t3) data points. Spectral widths were 7000 Hz in the F1 (^{13}C) dimension, 9124 Hz in the F2 (^{1}H) dimension, and 7000 Hz in the F3 (^{1}H) dimension.

Data were processed on Silicon Graphic Indigo workstations using XWINNMR (Bruker) and analyzed with FELIX 97.0 (MSI). Processing included apodization with a shifted squared sinebell window function, zero-filling, Fourier transformation, phasing, and baseline correction with fifth-order polynomials. The final two-dimensional data sets consisted of 1024 × 2048 real points (2048 × 8096 for DQF-COSY). Coupling constants were measured with a resolution of 0.7 Hz/point by evaluating the antiphase cross-peak separation on the DQF-COSY spectrum recorded at 288 K. For the three-dimensional F1 ^{13}C-edited−F3 ^{13}C-filtered HSQC NOESY, linear back-prediction of one data point and forward prediction of additional points were included in the processing. The final three-dimensional matrix consisted of 128 (F1) × 512 (F2) × 512 (F3) real points.

Scheme 3: Polymer-Supported Synthesis of PID-OH[a]

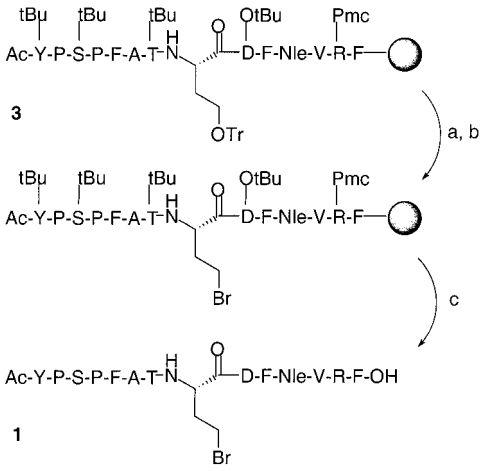

[a](a) TFA/triisopropylsilane/dichloromethane, 1/5/94; (b) $P(Ph)_3$/$CbBr_4$ in tetrahydrofuran; (c) TFA/water, 95/5.

High-Sensitivity Differential Scanning Calorimetry (HS-DSC). Calorimetric measurements were carried out with a high-sensitivity differential scanning microcalorimeter, VP-DSC (MicroCal Software, Inc., Northampton, MA), within the temperature range 15−105 °C, at the heating rate 60 °C/h and excess pressure of 2 atm (*38*). Protein concentrations were determined by spectrophotometry as mentioned above. DsbA concentration varied from 0.015 to 0.035 mM in the buffer 100 mM sodium phosphate, 1 mM EDTA, pH 7.0. Data processing was carried out with the software Origin 4.1 (MicroCal Inc.) and Kaleidagraph (Abelbeck).

RESULTS

PID-Br Synthesis. We developed a simple and straightforward solid-phase strategy for synthesizing large brominated peptides. This strategy is based on a two-step selective deprotection/bromination of the resin-bound peptide (Scheme 3). As a precursor of the brominated moiety, we used a protected homoserine to minimize side reactions. Commercial Fmoc-Hse(-trityl)-OH was employed because it allows a complete orthogonality of protections: the trityl group can be easily and selectively removed using 1% TFA in dichloromethane (*39*). After quantitative deprotection of *O*-trityl-homoserine, the resin-bound peptide was almost completely brominated using 10 equiv of both carbon tetrabromide and triphenylphosphine in tetrahydrofuran (*40, 41*). RP-HPLC analysis of the intermediary peptide obtained by cleavage of resin-bound PID-OH peptide revealed a major peak representing more than 94% of the total compounds. MALDI

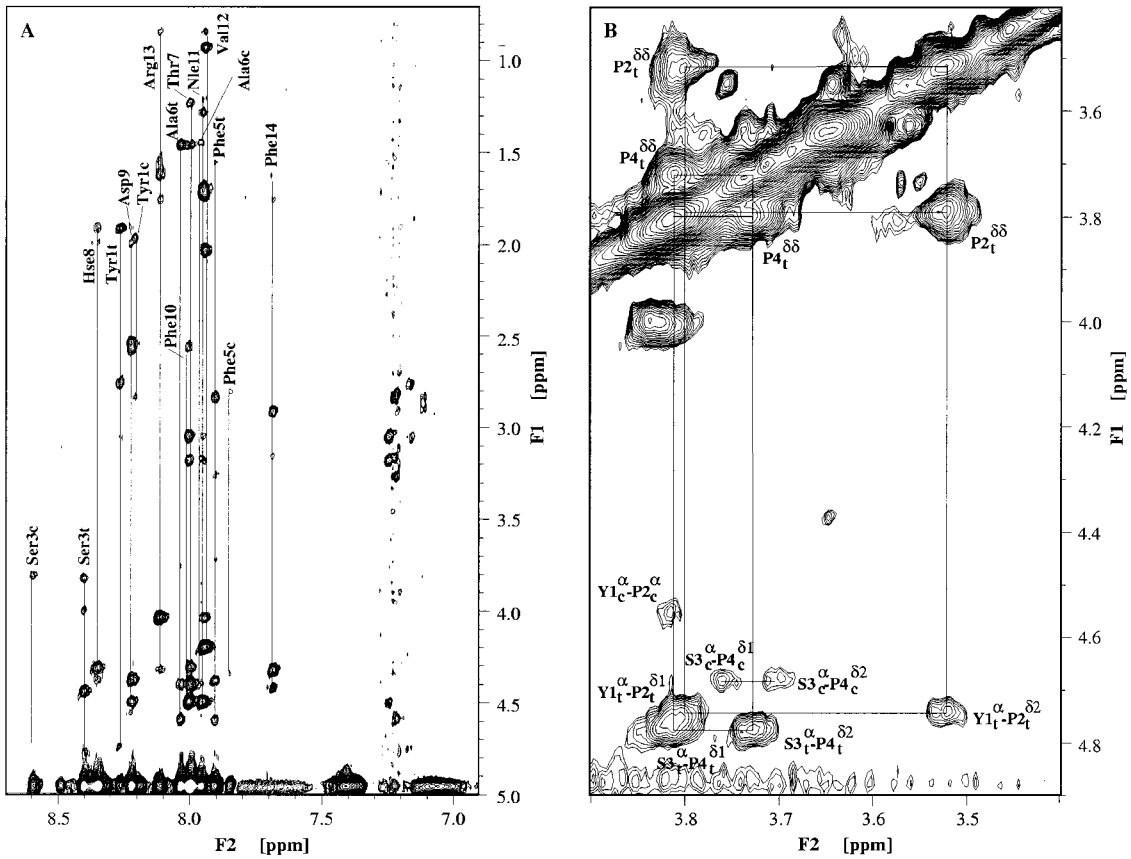

FIGURE 1: Sections of the NOESY spectrum of free PID-OH recorded in 40% CH_3OH/60% H_2O, 20 mM phosphate buffer, pH 5.8, at 288 K. (A) Amide-aromatic/aliphatic portion. Amide proton assignments are indicated with lines. (B) Aliphatic portion showing sequential NOEs between proline residues and their preceding neighbor. t and c denote the trans and cis isomer conformation of the Tyr_1-Pro_2 peptide bond, respectively.

mass spectrometry showed the presence of a single component (calculated $m/z = 1702.9$; observed $m/z = 1703.4$; MH^+), and sequencing by MS confirmed the expected sequence. Characterization of the crude brominated PID-Br peptide by MALDIMS revealed the expected molecular mass (calculated $m/z = 1765.8$; observed $m/z = 1766.1$).

The PID-Br peptide was found to be unstable in an aqueous environment. After one night at room temperature in 40% CH_3CN/H_2O, up to 70% of the peptide was degraded. The major degradation product was identified by ESIMS as the peptide resulting from the hydrolysis of the brominated moiety. In further biological experiments, PID-Br peptide was therefore solubilized in methanol just before use.

Spectroscopic Analyses on PID-OH. Since PID-Br is unstable in an aqueous environment, all the analyses have been performed on PID-OH. Prior to NMR analyses, the structure of the peptide was first checked by circular dichroism. Whatever the experimental conditions used (pH varying from 3.6 to 9, various concentrations of CH_3CN or CH_3OH in 20 mM sodium phosphate buffer, pH 5.8), no defined secondary structure could be observed.

The NMR analysis was performed in 20 mM sodium phosphate buffer, pH 5.8, which is usually used in our DsbA NMR studies (*31*). 40% CH_3OH was necessary to make soluble high concentrations of peptide. The sequence-specific assignments of PID-OH were achieved according to the standard method developed by Wüthrich and co-workers (*42*) and are provided as Supporting Information.

The weak dispersion of the ^{1}HN and ^{1}Hα signals observed in homonuclear spectra (Figure 1A) and the different NMR parameters confirm the circular dichroism analyses and demonstrate that the peptide is largely extended in solution. First, only sequential, and no medium-range, NOE connectivities were observed in both NOESY and ROESY spectra. These sequential NOE connectivities are characteristic of an extended conformation, i.e., strong ^{1}H$\alpha(i)-^1$HN$(i+1)$, weak to medium ^{1}H$\beta(i)-^1$HN$(i+1)$, and few weak ^{1}HN$(i)-^1$HN$(i+1)$ connectivities. Second, high $^3J_{HNH\alpha}$ coupling constants (between 7 and 9.5 Hz), which are typically found for residues in an extended conformation, were obtained for all amino acids. Finally, the lack of a region containing four contiguous residues exhibiting significant upfield/downfield ^{1}Hα shifts and opposite ^{13}Cα shifts relative to the random coil values also indicates the absence of secondary structure.

Two sets of resonances were observed for residues Tyr_1-Ala_6 on all homonuclear spectra, reflecting the existence of two distinct conformations in solution. The proportion of the major and minor conformations was estimated to be about 3/1, as determined from the relative intensities of the well-resolved aromatic resonances of Tyr_1 and amide resonances of Ser_3 arising from the two species. One phenomenon known to give rise to multiple sets of resonances in NMR spectra of peptides is *cis*−*trans* isomerism of the X−Pro peptide bond, because this process is slow on an NMR time scale (*43, 44*). In the major form, Pro_2 and Pro_4 are in the *trans* conformation as characteristic sequential NOEs (*42*) were seen between the ^{1}Hδ protons of Pro_2 and Pro_4 with

the $^1H\alpha$ of Tyr_1 and Ser_3, respectively (Figure 1B). In the minor form, Pro_2 is in the *cis* conformation as a sequential $^1H\alpha(i)-{}^1H\alpha(i+1)$ NOE was observed between Tyr_1 and Pro_2, whereas no NOE was found between Tyr_1 and $^1H\delta$ protons of Pro_2. For Pro_4, the same sequential NOEs were found in the minor and in the major form, demonstrating that only Pro_2 is subject to a slow *cis*−*trans* isomerization process.

Formation of the Covalent Complex DsbA−*PID.* After purification, DsbA is obtained essentially in its oxidized form and therefore has to be reduced prior to reaction with peptide PID-Br. The DTT used as reducing reagent was eliminated afterward to prevent any side reaction with the brominated peptide. In an aqueous reaction medium suitable for protein handling, the nucleophilic substitution of the Cys_{30} thiolate on PID-Br to form the complex competes with two other reactions: the reoxidation of the active site cysteines of DsbA and the hydrolysis of the brominated peptide. Moreover, the highly hydrophobic content of the peptide sequence makes it prone to aggregate. Both hydrolysis of the peptide and reoxidation of DsbA could be minimized by decreasing the pH of the reaction buffer to 5.5.

The hydrophobic PID-Br had to be solubilized in an organic solvent prior to any further use. CH_3OH was found to be compatible with both peptide and DsbA solubility. Far- and near-UV circular dichroism measurements showed no significant modification of the structural content of DsbA up to 50% CH_3OH added to the buffer. Complex formation and further dialysis steps were consequently performed in the presence of 30−40% CH_3OH in the medium.

The complex formation was performed at 4 °C to minimize the hydrolysis of PID-Br. With the same goal of minimizing the effect of peptide degradation, two successive additions of 2 equiv of brominated peptide were preferred to a unique addition of 4 equiv. After 24 h, the reaction appeared to reach a maximum around 60−80% substitution yield (Figure 2). The excess peptide was separated from the reaction mixture by dialysis against 20 mM sodium phosphate/40% CH_3OH. The separation of the complex from free DsbA proved to be more difficult because of the high similarity of their biophysical characteristics. They differed by only 1.7 kDa in their molecular mass and by the free thiol function in the reduced state of DsbA. Neither gel filtration or activated thiol-Sepharose chromatography, nor ionic exchange chromatography gave satisfactory results. A good separation of the unmodified DsbA and complex was finally obtained using hydrophobic chromatography on phenyl-Sepharose (Figure 2).

The two peaks obtained after hydrophobic chromatography were analyzed by ESIMS. The analysis of the first one revealed the presence of a single species (22 817.87 ± 1.13) whose molecular weight confirmed that the stoichiometric ratio of DsbA/peptide PID was 1/1 as expected (theoretical molecular weight = 22 816.87). The analysis of the second peak also revealed the presence of a single compound. Its molecular weight (21 131.33 ± 1.21) was in agreement with the theoretical value expected for unsubstituted DsbA.

Chemical Characterization of the DsbA−*PID Complex.* The first set of experiments aimed at demonstrating that the peptide was specifically bound to Cys_{30}. These data could not be easily obtained from proteolysis experiments and direct Edman sequencing due to the nature of the residues separating the two active site cysteines, i.e., Pro-His. This

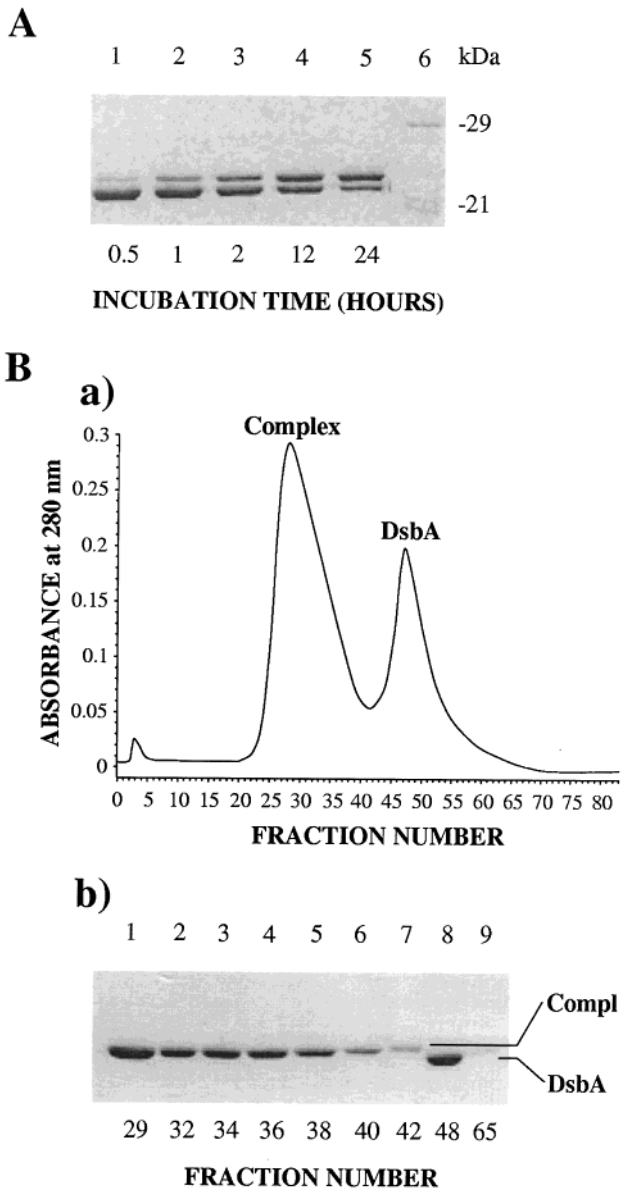

FIGURE 2: (A) Formation and (B) purification of the complex DsbA−PID. (A) Reduced DsbA (30 μM) in 20 mM phosphate buffer, pH 5.5/30% CH_3OH was incubated at 4 °C under argon with 2 equiv of the brominated peptide. Then 2 further peptide equiv was added after 3 h of incubation. Aliquots were withdrawn at different times after the first addition of the peptide and analyzed by 12% SDS−PAGE (lanes 1−5). Lane 6, molecular mass standards. (B) (a) Hydrophobic chromatography elution profile of the complexed and free DsbA mixture. The chromatography was performed at 4 °C on a phenyl-Sepharose HP column (Pharmacia Biotech) in 20 mM Tris-HCl buffer, pH 8, at a flow rate of 0.3 mL/min. Proteins were eluted with a linear gradient from 1 to 0.2 M ammonium sulfate in 165 min, followed by a plateau at 0.2 M ammonium sulfate during 35 min and a linear gradient from 0.2 to 0 M in 165 min. Fractions were collected every 5 min. (b) 12% SDS−PAGE analysis of the eluted fractions (lanes 1−9).

was achieved by means of carboxamidomethylation reactions and mass spectrometry analyses. After reaction with iodoacetamide, the number of free cysteines was determined from the mass increment of the protein. Moreover, the use of ESIMS enables the determination of the relative percentage of the modified proteic species present in solution thanks to their ion currents. This analysis is based on the assumption that the unmodified protein and its related carboxmethylated species are endowed with similar ionization capabilities. This

Table 1: Results of the Carboxamidomethylation (CAM) Experiments Performed on Oxidized DsbA (ox), Reduced DsbA (red), and Complexed DsbA (DsbA−PID) both in the Absence (−) and in the Presence (+) of 6 M Guanidinium Chloride

protein	mol wt determined by ESIMS	theoretical mol wt	no. of CAM	relative %
DsbA ox (−)	21131.62 ± 2.24	21130.07	0	100
DsbA ox (+)	21131.64 ± 1.10	21130.07	0	100
DsbA red (−)	21189.43 ± 2.61	21189.07	1	52
	21246.54 ± 1.95	21246.07	2	48
DsbA red (+)	21246.68 ± 1.85	21246.07	2	100
DsbA−PID (−)	22817.50 ± 1.84	22816.9	0	100
DsbA−PID (+)	22817.62 ± 2.5	22816.9	0	15
	22873.04 ± 2.6	22873.9	1	85

was previously demonstrated on several unrelated proteins (*45*−*47*).

The high selectivity of the alkylation with iodoacetamide toward cysteine residues of DsbA under our experimental conditions was checked on oxidized DsbA. After incubating DsbA with 10 molar excess of iodoacetamide over the number of cysteines, no modified residue could be detected by ESIMS. The alkylation experiments performed on reduced DsbA, in the absence of GdmCl, exhibited two proteic species (21 189.43 ± 2.61 and 21 246.54 ± 1.95). The former corresponded to DsbA with a single CAM (50%), the latter to DsbA with 2 CAM (50%). Although less reactive and less accessible to the solvent, the buried Cys_{33} partially reacts with iodoacetamide. This had also previously been observed by Zapun and co-workers (*48*). After complete denaturation in the presence of 6 M GdmCl, a unique species was detected that corresponded to DsbA with 2 CAM (21 246.68 ± 1.85) (Table 1). As expected, when the protein is fully denatured, both cysteines are made accessible to the alkylating reagent.

The ESIMS analysis of native DsbA−PID after reaction with iodoacetamide detected only the molecular weight corresponding to the unmodified complex (22 817.50 ± 1.84). The absence of carboxamidomethylation of the second cysteine as previously observed for DsbA may result either from steric hindrance due to the peptide or from a structural change in the neighborhood of the active site. After complete denaturation, we could observe the monosubstituted protein (22 873.04 ± 2.6) that represented 85% of the protein solution. From these experiments, we can deduce that nucleophilic substitution effectively occurred on a cysteine of the active site as expected. Although it is not unambiguously demonstrated, all data support the conclusion that the peptide is bound to the most accessible Cys_{30}. The second cysteine, Cys_{33}, seems less accessible to iodoacetamide in the complex than in the free protein as no modification occurred in the absence of GdmCl.

Insights into the Structure of the DsbA−PID Complex by NMR Analyses. Preliminary analyses performed by circular dichroism showed that the overall structure of DsbA was conserved when bound to the peptide (data not shown). The two-dimensional ^{1}H-^{15}N HSQC spectra of oxidized and complexed DsbA are shown in Figure 3. Their overall similarities demonstrate that the global fold of DsbA is not significantly affected upon peptide binding. In addition, no changes in ^{1}H-^{15}N HSQC spectra of the complex recorded at intervals of up to 3 months have been noticed, showing that the complex is stable and suitable for structural analyses. Significant differences in ^{1}HN and/or ^{15}N chemical shifts between free and peptide-bound DsbA spectra were observed for about 45 resonances (i.e., $\Delta\delta$ larger than 0.2 and 0.3 ppm for ^{1}HN and ^{15}N, respectively). These variations partly reflect changes in the electronic environment of some residues that occur upon disruption of the active site disulfide (*31*), but also likely interactions between DsbA and the bound peptide.

Isotope filtered experiments were performed to selectively observe the proton resonances of the unlabeled PID peptide (Figure 4). Figure 4A shows the fingerprint region of the isotope filtered [F1-C/N,F2-C/N]-NOESY spectrum of PID in the bound form. The large dispersion observed for the ^{1}HN and ^{1}Hα resonances suggests a structuration of the peptide in the complex. Inspection of the spectrum revealed that some spin systems split in two, with different intensities (e.g., at ^{1}HN frequencies = 9.34 and 9.27 ppm). This was also observed for a few resonances in the ^{1}H-^{15}N HSQC spectrum of the complex (e.g., at δ^1HN = 6.08 ppm, δ^{15}N = 109.0 ppm and at δ^1HN = 6.09 ppm, δ^{15}N = 111.9 ppm). The most probable explanation for these observations is that isomerization of the Tyr_1−Pro_2 peptide bond, already observed in the free peptide PID-OH, still occurs in the bound peptide. However, this process occurs in the N-terminal part of the peptide, which is not expected to interact strongly with DsbA. Therefore, it may not constitute a major problem for the study of interactions. The observation of two sets of resonances for some nuclei may also be due to the presence of two different positionings of the peptide at the surface of DsbA. To detect intermolecular NOEs between labeled DsbA and the unlabeled peptide, a F1 ^{13}C-edited−F3 ^{13}C-filtered HSQC NOESY experiment was carried out. Numerous intermolecular NOE cross-peaks are observed (Figure 4C) that involve several aromatic (labeled a and g) and aliphatic (e.g., c and d) residues of the peptide. These observations clearly demonstrate the presence of preferential noncovalent interactions between DsbA and the PID peptide.

HS-DSC Studies. The thermodynamic properties of the three forms of DsbA, i.e., oxidized, reduced, and complexed, were compared by DSC. The calorimetric curves obtained are shown in Figure 5. Transition temperatures (T_d) and variations of enthalpy (ΔH) for the denaturation reaction are reported in the inset table. The parameters obtained for reduced and oxidized states of the protein are in the error range of the values determined in previous studies performed under the same experimental conditions (*38*). All curves could be fitted according to a two-state model for unfolding. The denaturation transition of the complex occurred at T_d = 72.55 °C, an intermediate temperature between those of oxidized and reduced forms. The quantity of heat necessary to denature the complex (ΔH = 597.4 kJ/mol) was also between those required to denature oxidized and reduced forms (580.0 and 718.2 kJ/mol, respectively). The high background and baseline drifts in the fusion curves did not enable determination of the heat capacity increment (ΔC_p). The first studies performed on DsbA had already pointed out the difficulty of measuring this parameter (*38*). It was consequently not possible to compare precisely the difference of stability of the three forms of the protein (variation of ΔG). However, all our experiments suggest that the ΔC_p value for the complex was in the same range as the ΔC_p for both redox states [9.28 ± 2.09 kJ mol^{-1} K^{-1} in (*38*)].

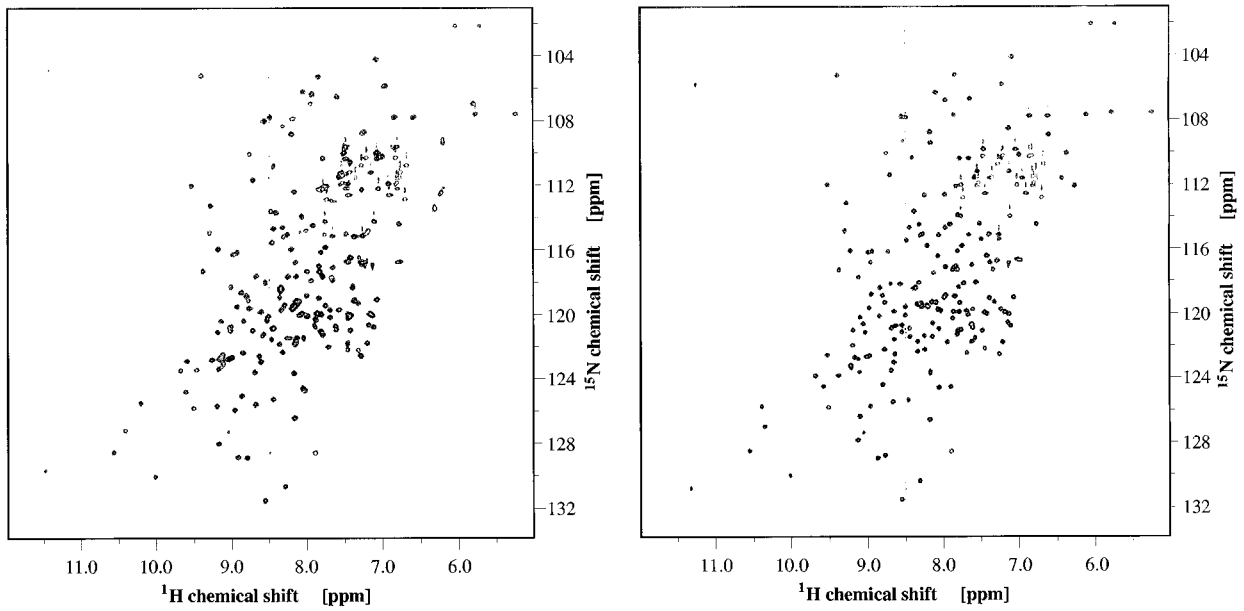

FIGURE 3: ^{1}H-^{15}N HSQC spectra of complexed (left panel) and oxidized (right panel) DsbA. Spectra were recorded at 600 MHz, 310 K, on 2 mM oxidized or peptide-bound DsbA in 90% H_2O/10% D_2O, 20 mM phosphate buffer, pH 5.8.

DISCUSSION

The preparation and the study of covalent complexes between peptidic substrates and thiol−disulfide oxidoreductases represent an important contribution to the understanding of the mechanism of disulfide−dithiol redox reactions in the cell. All the structural work published up to now on such complexes has been based on the use of enzyme variants for which the second active site cysteine was replaced by another residue. The NMR study of a complex between a C14S variant of glutaredoxin and its physiological substrate glutathione showed that the peptide was bound into a cleft of the protein (*49*, *50*). A covalent complex of human thioredoxin with a peptide deriving from nerve factor κB gave insights into the interaction between thioredoxin and this transcription factor (*51*). Other examples include complexes between human thioredoxin and a peptide from Ref-1 (*52*) and between glutaredoxin and a 25-mer from ribonucleotide reductase (*53*, *54*). As previously mentioned, this strategy was also applied to DsbA by reacting the variant C33A with a variant of RNase T1 (*14*). However, such an approach presents some limits, related in particular to the chemical stability of the disulfide linkage. The authors reported that the DsbA−RNase T1 complex was only stable for a few days (*14*). Furthermore, its high molecular weight has prevented any simple NMR analyses.

In the context of studying the mechanism of an enzyme, another limitation is related to the use of an enzyme variant. If we consider the case of DsbA (*14*), the first drawback of the C33A variant is the absence of the two redox states characteristic of the enzyme activity. The second major drawback is the difference in stability between the variant and the wild-type protein. C33A DsbA appears to be less stable than both redox forms of the wild-type enzyme [midpoints for the Gdm-Cl-induced unfolding/refolding transitions: 1.63 M for C33A (*14*) and 1.80 M/2.37 M for the oxidized and reduced states of DsbA, respectively (*55*)]. These properties do not allow direct comparison of the relative stabilities of the complexed and free forms of the protein. The chemical strategy developed in this work overcomes most of these inconveniences. We produced a stable mimic of a DsbA−ligand complex by reacting a bromohomoalanine-containing peptide with the wild-type enzyme. All the analyses performed on this species provide strong evidence that the ligand is specifically cross-linked to the active site cysteine Cys_{30}. The complex involving a thioether bridge proved to be stable in aqueous solution and could be used for structural studies under physiological conditions over several months. A first set of experiments has demonstrated its suitability for NMR analyses. In this context, it is noteworthy that this method has enabled the direct use of a wild-type isotope-labeled protein without requiring any mutagenesis, labeling, and purification of a suitable protein variant. Using appropriate experimental conditions, the approach could be applied to any peptidic sequence and any other protein or enzyme displaying an accessible and reactive cysteine in the ligand binding site. We have already successfully applied the chemical strategy to an unrelated peptide sequence containing hydrophilic residues, particularly Boc-lysine and trityl-histidine. Actually, most conventional protective groups proved resistant to the Hse deprotection and bromination, i.e., OtBu, tBu, Pmc, Boc, and trityl(His). The only residue that may require further investigation is methionine, which was substituted by a norleucine in our peptide. Only the presence of cysteine in the sequence is subject to precaution as it would certainly lead to the cyclization of the peptide by formation of a cystathionine moiety.

Biochemical studies of the interaction of DsbA with both peptidic (*8*) and proteic (*14*) substrates have suggested that DsbA interacts with its unfolded substrates not only by a covalent disulfide bond, but also by noncovalent interactions. According to the X-ray structure of oxidized DsbA, three uncharged surfaces surround the active site disulfide and could potentially participate in the binding of peptides (*7*). However, no structural evidence has yet been reported for such interactions. The NMR analysis of the free PID peptide showed that it is essentially unstructured in solution, and

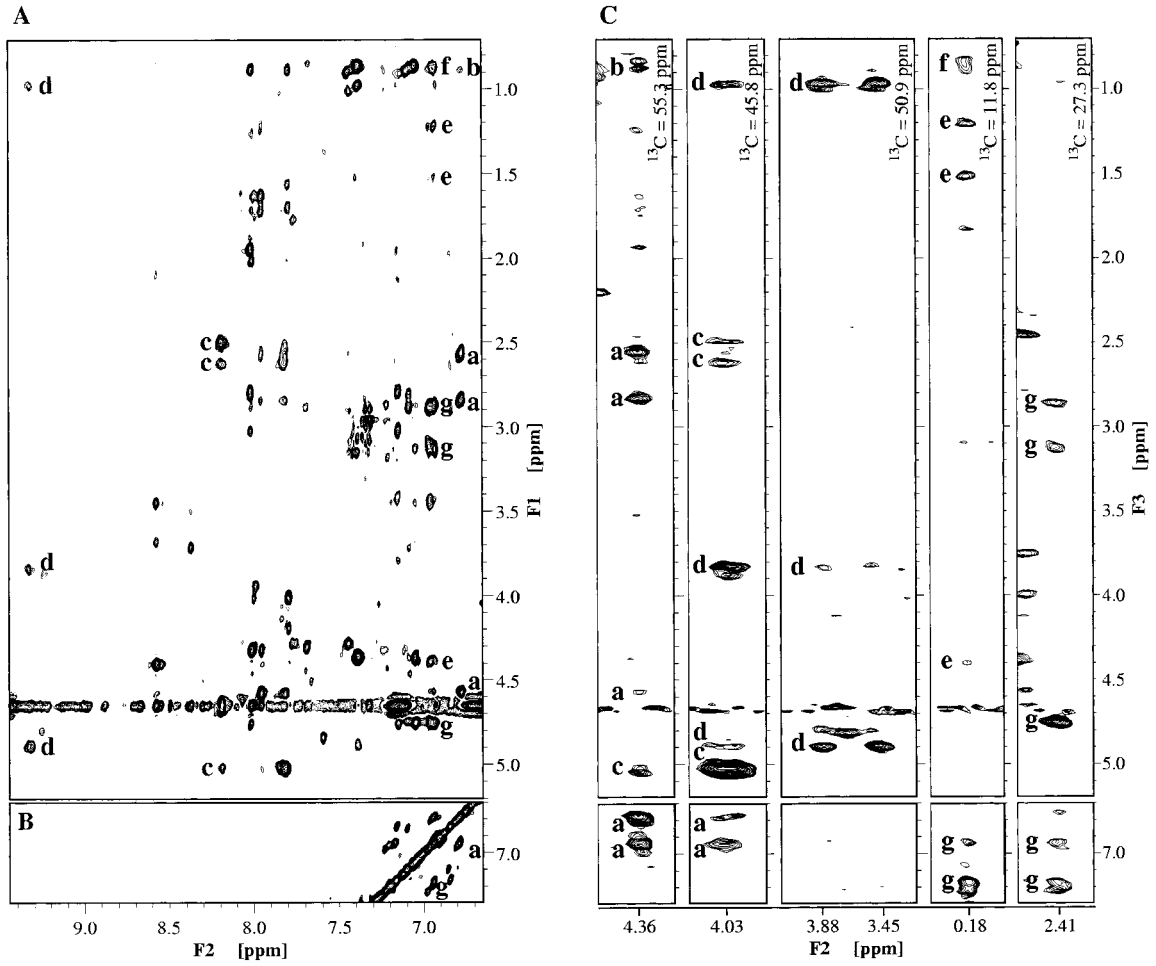

FIGURE 4: Portions of NOESY spectra recorded on the complex DsbA−PID between $^{13}C/^{15}N$-labeled DsbA and the unlabeled PID peptide. (A) Fingerprint region of the isotope filtered [F1-C/N,F2-C/N]-NOESY spectrum (*32*) showing intramolecular NOE cross-peaks between amide/aromatic and aliphatic protons of PID. The experiment was recorded on a 2 mM sample at 600 MHz, 310 K, in 90% H_2O/10% D_2O, 20 mM phosphate buffer, pH 5.8. (B) Aromatic region of the ^{13}C double-tuned [F1,F2] pulsed-field gradient z-filtered NOESY (*33*) showing intramolecular NOEs between aromatic protons of the bound peptide. The complex was dissolved in 100% D_2O, 20 mM phosphate buffer, pH 5.8. The experiment was recorded at 600 MHz, 310 K. (C) Strip plots of the three-dimensional F1 ^{13}C-edited−F3 ^{13}C-filtered HSQC-NOESY spectrum (*33, 34*) showing intermolecular NOE signals between aromatic/aliphatic protons of PID and aliphatic protons of DsBA. The spectrum was recorded at 800 MHz, 310 K, on the sample dissolved in 100% D_2O. Letters represent some proton spin systems of PID for which intermolecular NOEs with protons of DsbA are observed in (C).

can consequently by considered as a part of an unfolded protein. The preliminary NMR experiments carried out on the DsbA−PID complex show numerous intermolecular NOE cross-peaks which demonstrate the existence of noncovalent interactions. More detailed NMR analyses using additional heteronuclear edited and filtered techniques are currently in progress. They will help to define the precise nature and extent of these interactions as well as the areas of DsbA involved in the binding of the substrates. Nevertheless, several conclusions can be drawn about the strength of these interactions. Thermal unfolding experiments are good sensors of significant protein−ligand interactions because these interactions induce change in transition temperatures. We wondered whether the PID sequence contains any determinants for the interaction with DsbA in the absence of covalent cross-linking. Thus, we incubated increasing concentrations of PID-OH peptide with oxidized DsbA, which is the redox form that interacts with the substrates, and performed DSC measurements. Whatever the ratio used (up to 50 equiv), no significant variation in the T_d temperature could be detected compared to the value obtained for oxidized DsbA (data not shown). The first conclusion is that interactions between DsbA and PID-OH are relatively weak. This is consistent with the role of DsbA as a nonspecific oxidase. The noncovalent interactions between DsbA and unfolded proteins have to be not too strong to avoid the formation of inhibitory complexes. A possible explanation for the lack of affinity of PID-OH is the absence of chemical reactivity with the active thiol of DsbA. We synthesized the thiol form of the peptide (PID-SH) that displays a Cys residue in place of the homoserine. A proportional increase of fluorescence signals could be detected when DsbA is equilibrated with increasing concentrations of PID-SH (ranging from 1/1 to 1/50 DsbA/PID-SH molar ratio). However, as with the PID-OH peptide and although the effect is larger, the fluorescence experiments did not allow us to measure confidently a binding equilibrium constant. An additional problem in the case of the PID-SH peptide was that we could not discriminate between the consequence of the reduction of DsbA and the consequence of the binding per se. This very preliminary result suggests that the nucleophilic attack of the DsbA disulfide is an important prerequisite to the formation of strong noncovalent interactions that will stabilize the complex.

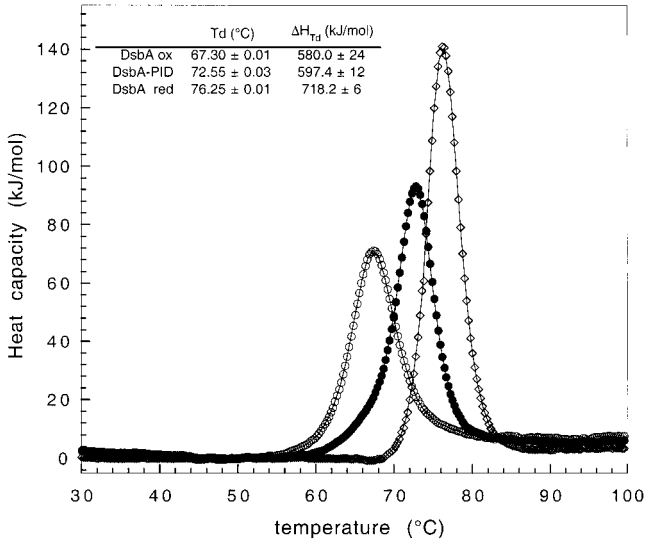

FIGURE 5: Excess heat capacity curves for oxidized (○), complexed (●), and reduced (◇) forms of DsbA. All thermal transitions could be fitted according to a two-state model, and both ΔH and T_d values were calculated after corrections of the baseline at high temperatures (inset).

Thermodynamic experiments provided additional insights into the mechanism of DsbA-mediated oxidation reactions. In the absence of well-defined ΔC_p values, it was not possible to measure strictly the free energies for the three forms of the protein. However, our results suggested a ΔC_p value for the complex in the same range as the values previously measured for both redox states (*38*). In that case, the ΔG values calculated for the complex with ΔC_p ranging from 6 to 10 kJ mol^{-1} K^{-1} are always between the variations in free energy determined for oxidized and reduced forms. This confirms what could be suspected from the T_d values: this is the first evidence that the formation of the mixed-disulfide intermediate thermodynamically stabilizes the protein compared to its original oxidized state. The second step of the DsbA-catalyzed reaction, that releases the oxidized substrate and reduced DsbA, results in a third form of the enzyme even more stable than the two previous ones. The molecular determinants of the increasing stability along the DsbA catalysis (downward thermodynamic process) are not obvious. The presence of interactions between the ligand and the protein constitutes a factor of stabilization of the complexed form compared to the oxidized one. Another factor may be the release of the strain associated with the intramolecular disulfide. The highest stabilization happens in the reduced form and may be related to the presence of the free thiolate at position 30. Indeed, both crystallography and NMR analyses of oxidized and reduced DsbA showed no major structural changes that could explain the variation in stability (*31, 56, 57*). Both protein electrostatics and dynamics might contribute significantly to the changes observed, but they are difficult to address experimentally. This report opens the way to the structure and dynamics of a DsbA−peptide ligand and to the subsequent modeling of the complete catalytic cycle of DsbA.

ACKNOWLEDGMENT

We thank Yvan Choiset and Thomas Haertlé for their skillful assistance in DSC analyses, Jean-Baptiste Charbonnier, Nadège Jamin, and Catherine Vialle-Printems for fruitful discussion, Régine Romy-Lebrun, Gilles Mourier, and Agathe Urvoas for technical help, and David McCarthy for checking the English of the manuscript.

SUPPORTING INFORMATION AVAILABLE

Resonance assignments and $^3J_{HNH\alpha}$ coupling constants of the PID-OH peptide at 288 K in 40% CD_3OH/60% H_2O, 20 mM phosphate buffer, pH 5.8 (2 pages). This material is available free of charge via the Internet at http://pubs.acs.org.

REFERENCES

1. Freedman, R. B. (1995) *Curr. Opin. Struct. Biol. 5*, 85−91.
2. Creighton, T., Zapun, A., and Darby, N. (1995) *Trends Biotechnol. 13*, 18−23.
3. Raina, S., and Missiakas, D. (1997) *Annu. Rev. Microbiol. 51*, 179−202.
4. Creighton, T. E., and Freedman, R. B. (1993) *Curr. Biol. 3*, 790−793.
5. Chivers, P. T., Laboissiere, M. C., and Raines, R. T. (1996) *EMBO J. 15*, 2659−2667.
6. Martin, J. L., Bardwell, J. C., and Kuriyan, J. (1993) *Nature 365*, 464−468.
7. Guddat, L. W., Bardwell, J. C. A., Zander, T., and Martin, J. L. (1997) *Protein Sci. 6*, 1148−1156.
8. Darby, N. J., and Creighton, T. E. (1995) *Biochemistry 34*, 3576−3587.
9. Wunderlich, M., and Glockshuber, R. (1993) *Protein Sci. 2*, 717−726.
10. Nelson, J. W., and Creighton, T. E. (1994) *Biochemistry 33*, 5974−5983.
11. Bardwell, J., Lee, J.-O., Jander, G., Martin, N., Belin, D., and Beckwith, J. (1993) *Proc. Natl. Acad. Sci. U.S.A. 90*, 1038−1042.
12. Guilhot, C., Jander, G., Martin, N. L., and Beckwith, J. (1995) *Proc. Natl. Acad. Sci. U.S.A. 92*, 9895−9899.
13. Kishigami, S., Kanaya, E., Kikuchi, M., and Ito, K. (1995) *J. Biol. Chem. 270*, 17072−17074.
14. Frech, C., Wunderlich, M., Glockshuber, R., and Schmid, F. X. (1996) *EMBO J. 15*, 392−398.
15. Lin, S.-R., Chang, L.-S., and Chang, C.-C. (1999) *Biochem. Biophys. Res. Commun. 254*, 104−108.
16. Nakamura, K., Era, S., Ozaki, Y., Sogami, M., Hayashi, T., and Murakami, M. (1997) *FEBS Lett. 417*, 375−378.
17. Dugave, C., and Ménez, A. (1997) *Tetrahedron Asymm. 8*, 1453−1465.
18. Mayer, J., Zhang, J., Groeger, S., Liu, C., and Jarosinski, M. (1998) *J. Pept. Res. 51*, 432−436.
19. Sieber, P., and Riniker, B. (1987) *Tetrahedron Lett.*, 6031−6034.
20. Davis, A. L., Laue, E. D., Keeler, J., Moskau, D., and Lohman, J. (1991) *J. Magn. Reson. 94*, 637−644.
21. Cavanagh, J., and Rance, M. (1990) *J. Magn. Reson. 88*, 72−85.
22. Shaka, A. J., Lee, C. J., and Pines, A. (1988) *J. Magn. Reson. 77*, 274−293.
23. Kumar, A., Ernst, R. R., and Wüthrich, K. (1980) *Biochem. Biophys. Res. Commun. 95*, 1−6.
24. Desvaux, H., Berthault, P., Birlirakis, N., and Goldman, M. (1993) *J. Magn. Reson. A108*, 219−229.
25. Desvaux, H., Berthault, P., Birlirakis, N., Goldman, M., and Piotto, M. (1995) *J. Magn. Reson. A113*, 47−52.
26. Kay, L. E., Keifer, P., and Saarinen, T. (1992) *J. Am. Chem. Soc. 114*, 10663−10665.
27. Grzesiek, S., and Bax, A. (1993) *J. Biomol. NMR 3*, 185−204.
28. Wishart, D. S., Sykes, B. D., and Richards, F. M. (1992) *Biochemistry 31*, 1647−1651.
29. Wishart, D. S., and Sykes, B. D. (1994) *J. Biomol. NMR 4*, 171−180.
30. Wishart, D. S., Colin, G. B., Holm, A., Hodges, R. S., and Sykes, B. D. (1995) *J. Biomol. NMR 5*, 67−81.

31. Couprie, J., Remerowski, M., Bailleul, A., Courçon, M., Gilles, N., Quéméneur, E., and Jamin, N. (1998) *Protein Sci. 7*, 2065−2080.
32. Ikura, M., and Bax, A. (1992) *J. Am. Chem. Soc. 114*, 2433−2440.
33. Ogura, K., Terasawa, H., and Inagaki, F. (1996) *J. Biomol. NMR 8*, 492−498.
34. Zwahlen, C., Legault, P., Vincent, S. J. F., Greenblatt, J., Konrat, R., and Kay, L. E. (1997) *J. Am. Chem. Soc. 119*, 6711−6721.
35. Piotto, M., Saudek, V., and Sklenar, V. (1992) *J. Biomol. NMR 2*, 661−665.
36. Shaka, A. J., Barker, P. B., and Freeman, R. (1985) *J. Magn. Reson. 64*, 547−552.
37. Marion, D., Ikura, M., Tschudin, R., and Bax, A. (1989) *J. Magn. Reson. 85*, 393−399.
38. Moutiez, M., Burova, T., Haertlé, T., and Quéméneur, E. (1999) *Protein Sci. 8*, 106−112.
39. Barlos, K., Gatos, D., Koutsogianni, S., Schafer, W., Stavropoulos, G., and Wenqing, Y. (1991) *Tetrahedron Lett. 32*, 471−474.
40. Rabinowitz, R., and Marcus, R. (1962) *J. Am. Chem. Soc. 84*, 1312−1313.
41. Ramirez, F., Desai, N., and McKelvie, N. (1962) *J. Am. Chem. Soc. 84*, 1745−1747.
42. Wüthrich, K. (1986) *NMR of proteins and nucleic acids*, John Wiley & Sons, Inc., New York.
43. Grathwohl, C., and Wüthrich, K. (1976) *Biopolymers 15*, 2025−2041.
44. Grathwohl, C., and Wüthrich, K. (1981) *Biopolymers 20*, 2623−2633.
45. Ruoppolo, M., Freedman, R. B., Pucci, P., and Marino, G. (1996) *Biochemistry 35*, 13636−13646.
46. Ruoppolo, M., Lundström-Ljung, J., Talamo, F., Pucci, P., and Marino, G. (1997) *Biochemistry 36*, 12259−12267.
47. Ruoppolo, M., Moutiez, M., Mazzeo, M., Pucci, P., Ménez, A., Marino, G., and Quéméneur, E. (1998) *Biochemistry 37*, 16060−16068.
48. Zapun, A., Bardwell, J. C., and Creighton, T. E. (1993) *Biochemistry 32*, 5083−5092.
49. Bushweller, J., Billeter, M., Holmgren, A., and Wüthrich, K. (1994) *J. Mol. Biol. 235*, 1585−1597.
50. Nordstrand, K., Aslund, F., Holmgren, A., Otting, G., and Berndt, K. (1999) *J. Mol. Biol. 286*, 541−552.
51. Qin, J., Clore, G. M., Kennedy, W. M., Huth, J. R., and Gronenborn, A. M. (1995) *Structure 3*, 289−297.
52. Qin, J., Clore, G., Kennedy, W., Kuszewski, J., and Gronenborn, A. (1996) *Structure 4*, 613−620.
53. Berardi, M., Pendred, C., and Bushweller, J. (1998) *Biochemistry 37*, 5849−5857.
54. Berardi, M., and Bushweller, J. (1999) *J. Mol. Biol. 292*, 151−161.
55. Hennecke, J., Spleiss, C., and Glockshuber, R. (1997) *J. Biol. Chem. 272*, 189−195.
56. Guddat, L., Bardwell, J., and Martin, J. (1998) *Curr. Biol. 6*, 757−767.
57. Schirra, H., Renner, C., Czisch, M., Huber-Wunderlich, M., Holak, T., and Glockshuber, R. (1998) *Biochemistry 37*, 6263−6276.

BI992873F